Luminescence of quartz and feldspar fingerprints provenance and correlates with the source area denudation in the Amazon River basin

Sawakuchi, A.O.; Jain, M.; Mineli, T.D.; Nogueira, F.; Bertassoli, D.J.; Häggi, C.; Sawakuchi, H.O.; Pupim, F.N.; Grohmann, C.H.; Chiessi, C.M.

Total number of authors:
14

Published in:
Earth and Planetary Science Letters

Link to article, DOI:
10.1016/j.epsl.2018.04.006

Publication date:
2018

Document Version
Peer reviewed version

Luminescence of quartz and feldspar fingerprints provenance and correlates with the source area denudation in the Amazon River basin

Sawakuchi[1*], A.O., Jain[2], M., Mineli[1], T.D., Nogueira[1], L., Bertassoli Jr.[1], D.J., Häggi[3], C., Sawakuchi[4,5], H.O., Pupim[6], F.N., Grohmann[7], C.H., Chiessi[8], C.M., Zabel[3], M., Mulitza[3], S., Mazoca[1], C.E.M., Cunha[1], D.F.

[1]Institute of Geosciences, University of São Paulo, Rua do Lago, 562, São Paulo, SP, Brazil.

[2]Center for Nuclear Technologies, Technical University of Denmark, DTU Risø Campus, DK-4000 Roskilde, Denmark.

[3]MARUM-Center for Marine Environmental Sciences, University of Bremen, Leobener Straße 8, D-28359 Bremen, Germany.

[4]Environmental Analysis and Geoprocessing Laboratory, Center for Nuclear Energy in Agriculture, University of São Paulo, Av. Centenário, 303, Piracicaba, SP, Brazil.

[5]Department of Ecology and Environmental Science, Umeå Universitet.
KBC-huset, Linnaeus väg 6, 901 87 Umeå, Sweden.

[6]Department of Environmental Sciences, Federal University of São Paulo, Rua São Nicolau, 210, Diadema, SP, Brazil.

[7]Institute of Energy and Environment, University of São Paulo, Av. Prof. Luciano Gualberto 1289, São Paulo, SP, Brazil.

[8]School of Arts, Sciences and Humanities, University of São Paulo, Av. Arlindo Bettio 1000, São Paulo, SP, Brazil.

*Corresponding author: Institute of Geosciences, University of São Paulo, Rua do Lago, 562, São Paulo, SP, Brazil, 05508-080 - Phone: +55-11-3091-0496 - Email: andreos@usp.br

Keywords: sediment provenance, luminescence, denudation, tropical rivers, Amazon

Abstract

The Amazon region hosts the world's largest watershed spanning from high elevation Andean terrains to lowland cratonic shield areas in tropical South America. This study explores variations in optically stimulated luminescence (OSL) and infrared stimulated luminescence (IRSL) signals in suspended silt and riverbed sands retrieved from major Amazon rivers. These rivers drain Pre-Cambrian to Cenozoic source rocks in areas with contrasting denudation rates.

In contrast to the previous studies, we do not observe an increase in the OSL sensitivity of quartz with transport distance; for example, Tapajós and Xingu Rivers show more sensitive quartz than Solimões and Madeira Rivers, even though the latter have a significantly larger catchment area and longer sediment transport distance. Interestingly, high sensitivity quartz is observed in rivers draining relatively stable Central Brazil and Guiana shield areas (denudation rate ξ = 0.04 mm.yr^{-1}), while low sensitivity quartz occurs in less stable Andean terrains (ξ = 0.24 mm.yr^{-1}). An apparent linear correlation between quartz OSL sensitivity and denudation rate suggests that OSL sensitivity may be used as a proxy for erosion rates in the Amazon basin. Furthermore, luminescence sensitivity measured in sand or silt arises from the same mineral components (quartz and feldspar) and clearly discriminates between Andean and shield sediments, avoiding the grain size bias in provenance analysis. These results have implications for using luminescence sensitivity as a proxy for Andean and shield contributions in the stratigraphic record, providing a new tool to reconstruct past drainage configurations within the Amazon basin.

1. Introduction

Large tropical rivers promote the transfer of rock weathering products to oceans (Latrubesse et al. 2005), representing an important component of the Earth surface system. The Amazon River is the world's largest river draining an area of 6.15 x 10^6 km^2, with average annual water discharge of 200,000 m^3.s^{-1} (Meade, 1994). The tributaries of the Amazon River mainly drain the Guiana shield and Central Brazil shield, with the headwaters of some western Amazon rivers flowing through the Andes mountain belt. Gibbs (1967) estimated that 82% of

the suspended sediments transported by the modern Amazon River come from Andean zones representing only 12% of the Amazon River basin. According to Filizola and Guyot (2009), total suspended sediment yield from Andean areas is more than 10^9 t.yr^{-1} while the maximum total suspended sediment yield of shield areas is only 10^8 t.yr^{-1}. This decoupling between suspended sediment load and drainage area arises from contrasting erosion rates in catchments draining the Andes and the cratonic shield areas. This contrast is also observed for the production of total dissolved solids transported by Amazon rivers. Andean tributaries contribute with around 64% of total dissolved solids delivered by the Amazon River to the Atlantic Ocean (Moquet et al., 2016). According to Wittmann et al. (2010) erosion rates in the Andes (0.5 mm.yr^{-1}) are one to two orders of magnitude higher than the erosion rates in Guiana and Central Brazil shields (0.01 mm.yr^{-1}). Most of the studies regarding the origin and transport of sediments in the Amazon fluvial system focused on fine-grained suspended sediments (Meade, 1994; Guyot et al., 2007; Viers et al., 2008) or dissolved solids (Moquet et al., 2016) and little is known about the sources and transport of bedload sands and their coupling to suspended sediments on a basin-wide scale. Furthermore, the relative contribution of sediments transported by tributaries of the Solimões River, which has large Andean and lowland tributaries, is poorly constrained. Suspended and bedload sediments transported and stored within the Amazon River system support the development of flooding forest substrates and its specific biodiversity (McClain and Naiman, 2008). Sediments from the Amazon River accumulated in the equatorial Atlantic Ocean are also important archives to reconstruct past changes in Amazon precipitation (Govin et al., 2014) and landscape (Dobson et al., 2001). Thus, understanding sediment sources and transport-storage routes in the Amazon River system is critical to any reconstruction of past conditions of the Amazon climate and its fluvial system.

Diverse properties of terrigenous sediments like major elements geochemistry (e.g. Govin et al., 2012) and heavy minerals suites (e.g. Morton and Hallsworth, 1999) have been used in sediment provenance analysis. However, sediment provenance analysis based on elemental geochemistry can be influenced by grain size (Bouchez et al., 2011) while minor components like heavy minerals can promote bias toward source rock types rich in specific

heavy minerals more resistant to weathering processes (Morton and Hallsworth, 1999). Isotopic analysis such as neodymium and strontium isotopes (Viers et al., 2008), while being relatively robust, are rather expensive and not available in most laboratories. Thus, it becomes imperative to search for other innovative approaches to provenance analysis, which are robust, inexpensive and easily accessible. It has been demonstrated in the past that the optically stimulated luminescence (OSL) may be used for provenance fingerprinting (Sawakuchi et al., 2012; Lü et al., 2014). In particular, the OSL sensitivity (emission intensity per unit mass per unit radiation dose) of quartz grains may be related to the source and transport history (i.e. deposition-erosion cycles) of sediments (Preusser et al., 2006; Pietsch et al., 2008; Juyal et al., 2009; Sawakuchi et al., 2011; Gliganic et al., 2017). In this study, we use OSL signals of quartz and infrared stimulated luminescence (IRSL) signals of feldspar to characterize the sources of suspended and riverbed sediments in the major tributaries of the Amazon main stem, namely the Solimões, Negro, Madeira, Tapajós and Xingu Rivers. The sources of sediments transported by the Solimões River, which is named as Amazon River after meeting the Negro River, is distinguished by the analysis of sediments from its major tributaries, including the Içá, Japurá, Jutaí, Juruá, Tefé, Urucu (Coari) and Purus Rivers. This study has general implications for provenance reconstructions in tropical settings since quartz and feldspar, which dominate the luminescence signals of sediments, are major components of terrigenous sediments.

2. The Amazon fluvial system

The modern Amazon fluvial system drains the equator between about 5°N to 15°S, placing the Amazon basin in the wet tropics, a region defined by relatively high precipitation (>1,500 mm.yr^{-1}) and temperature (>20°C) (Silva et al., 2011). Besides covering this large latitudinal range, the Amazon drainage basin extends longitudinally across 3,000 km, connecting the Andes mountain belt, Guiana shield and the Central Brazil shield with the equatorial Atlantic Ocean. This relief configuration and large latitudinal range induce high spatial variability of rainfall in the Amazon drainage basin (Espinoza Villar et al., 2009). After reaching the shore of the equatorial Atlantic Ocean, the Amazon River sediments are

transported northwestward by the North Brazil Current and are deposited on the northern South American continental margin giving rise to prominent features like the Guiana mud belt and the sub-aqueous Amazon delta (Nittrouer et al., 1995). The Amazon rivers drain regions with contrasting relief and erosion rates (Wittmann et al., 2010) as well as with variable rock types, including Pre-Cambrian igneous and metamorphic rocks in shield areas, Cenozoic metasedimentary and volcanic rocks in Andes and Paleozoic-Mesozoic sedimentary and igneous rocks in lowland Amazonia (Jaillard et al., 2000; Tassinari et al., 2000). This diverse geological scenario assigns different characteristics to the Amazon rivers, which are classified regarding the water type in white, black and clear water rivers (Sioli, 1984). White water rivers have high suspended load and dissolved solids, and neutral to alkaline waters; they are represented by rivers with headwaters draining the Andes mountains such as the Madeira, Solimões, and Içá Rivers (Figure 1). Black water rivers have low suspended load, high concentration of organic dissolved compounds and acidic waters; the Negro River draining the Guiana shield is the major Amazon black water river. Clear water rivers have low suspended load and acidic to slightly alkaline waters (Sioli, 1984). The Xingu and Tapajós Rivers, which drain the Central Brazil shield are the major Amazon clear water rivers.

The Solimões River, formed by the confluence of the Marañón and Ucayali Rivers, and the Madeira River, are the main Andean tributaries of the Amazon River; the upper reaches of these rivers drain the Andean highlands (> 3,000 m), while their lower reaches flow through Amazon lowlands (< 200 m). The Solimões and Madeira Rivers drain areas of ~2,150,000 km^2 and ~1,360,000 km^2, respectively and contribute around 90% of the total suspended load transported by the Amazon River (Latrubesse et al., 2005). The Negro River drains an area of approximately 700,000 km^2, mainly flowing through the Guiana shield on areas with elevation lower than 200 m until it reaches the Solimões River to form the Amazon River. The Tapajós and Xingu Rivers are the main tributaries of the Amazon River in eastern Amazon. The area of the Tapajós and Xingu drainage basins are around 500,000 km^2, emplaced on medium altitude terrains (30-700 m) of the Central Brazil shield. The Negro, Tapajós and Xingu Rivers have

very low sediment yield compared to the Solimões and Madeira Rivers (Latrubesse et al., 2005).

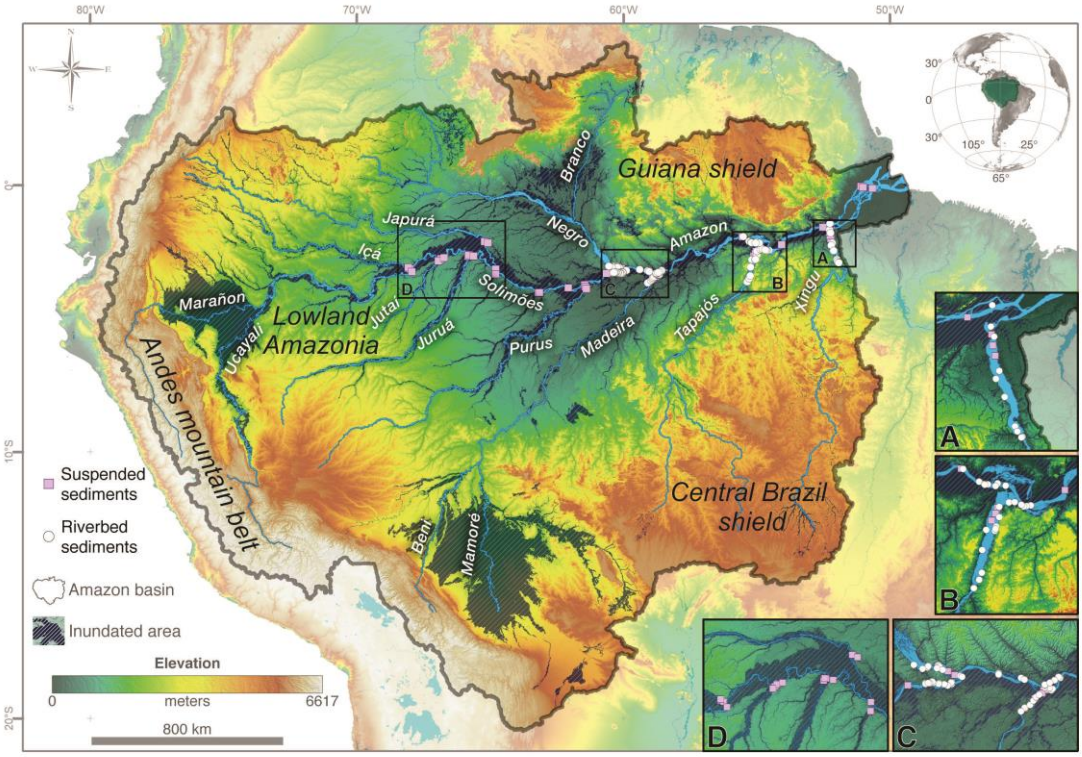

Figure 1. Sediment sampling sites in the Amazon fluvial system. Major geomorphological domains are represented by the Andes mountain belt, Guiana shield, Central Brazil shield and lowland Amazonia, which define areas with different elevations.

3. Methods

3.1. Sediment sampling

Riverbed and suspended sediments were collected in downstream sectors of the Solimões, Negro, Madeira, Tapajós and Xingu Rivers and along the Amazon main stem. Additionaly, suspended sediments samples were also collected in the downstream sectors of the major tributaries of the Solimões River, which included the Içá, Japurá, Jutaí, Juruá, Tefé, Urucu-Coari and Purus Rivers, as well as in the Solimões-Amazon main stem between the mouths of the Içá and Xingu Rivers (Figure 1). The sampling surveys were carried out during periods of low water level in September of 2011 and October-November of 2015 and during a period of high water level in May of 2012. Riverbed sand samples were retrieved from bar tops

156 exposed during the low water level periods or using a grab sampler in underwater channel
157 zones; these range from nine (Negro) to 25 (Amazon) samples collected per river. Suspended
158 sediments were retrieved at 2/3 water column depth or at three different depths of 1 m, 2/3
159 water column depth and 1-2 m above riverbed. Water collected with a submersible pump was
160 filtered using acetate cellulose filters (0.2 µm) for concentration of sediments for inorganic
161 geochemistry analysis (250 to 1000 ml of water per filter). Filters with suspended sediments
162 were dried (40ºC) immediately after water filtration. For luminescence measurements in
163 suspended sediments, larger volumes of water (40-60 l) sampled during October-November of
164 2015 were used to concentrate fine-grained sediments (> 0.45 µm) using a membrane
165 ultrafiltration system coupled to a peristaltic pump. Suspended sediments for inorganic
166 geochemistry analysis were sampled in three sites per studied river during the low and high
167 water level periods. The only exception was the Xingu River, with four sampling sites per water
168 level period.

169 The catchment area upstream sampling sites and channel length from sampling sites to
170 river springs were estimated using digital elevation models. These data allowed to evaluate
171 variations in luminescence sensitivity along sediment transport routes and to test the hypothesis
172 that sediment transport drives the sensitization of quartz in the Amazon fluvial system.

173

174 **3.2. Luminescence measurements**

175 The riverbed sand samples were wet sieved to isolate the 180–250 µm grain size fraction,
176 which is a grain-size fraction representing bed load sediments in the studied samples and it is
177 suitable for luminescence measurements in multigrain aliquots. Lithium metatungstate solution
178 (density 2.85 g/cm^3) was used to separate light (feldspar and quartz) from heavy minerals. Tests
179 using hydrochloric acid (HCl 10%) showed the absence of carbonate minerals. Organic matter
180 was eliminated using hydrogen peroxide (H_2O_2). Thus, the preparation of polymineral sand
181 grains only included HCl and H_2O_2 treatments, without application of hydrofluoric (HF) acid
182 etching. Three to six riverbed samples from each river were selected for preparation of pure
183 quartz fraction through HF acid treatment (38% HF for 40 min) of the lighter fraction. Infrared

stimulation (IR) was performed to confirm the absence of feldspar contamination in the HF treated quartz fraction. Samples with remaining feldspar were subjected to steps of HF 5% etching for 24 hours followed by wet sieving (180 µm), with IR signal checked after each step, until complete elimination of feldspar grains.

The suspended sediment samples were centrifuged to eliminate water excess and increase sediment concentration. Grain size separation and chemical treatments were not performed with suspended sediment samples to avoid sediment loss. Grain size analyses were performed to characterize the silt fractions dominating the suspended sediment samples, using a Mastersizer 2000 laser diffraction particle size analyzer (Malvern Instruments). Sediment samples were dispersed in deionized water for measurement. Grain size (0.1-1000 µm) distributions show that the fine to medium silt (7-30 µm) dominate the majority of the analyzed suspended sediments. A small number of samples have modes in the very fine to fine silt fraction (4-15 µm) or in the medium to coarse silt fraction (15-62 µm). The amount of sand ranges from 0.4 to 49.9%, but 90% of the suspended sediment samples have less than 16% of sand. Higher concentrations of sand only occur in samples collected at depths near the riverbed.

Luminescence measurements were performed in the Luminescence and Gamma Spectrometry Laboratory at the Institute of Geosciences of the University of São Paulo using polymineral (quartz and feldspar) aliquots and quartz aliquots of fine sand (180–250 µm) or polymineral aliquots of silt (4-62 µm). Measurements were performed in a Risø TL/OSL DA-20 reader equipped with a built-in beta source ($^{90}Sr/^{90}Y$; dose rate of 0.088 $Gy.s^{-1}$ for cups and 0.108 $Gy.s^{-1}$ for discs), a bialkali PM tube (Thorn EMI 9635QB), a sample heater plate, and blue and IR light emitting diodes (LEDs). Aliquots were measured using the blue LED's and light detection through a 7.5 mm Hoya U-340 glass filter (290–340 nm). For sand sized grains, about 12 aliquots per sample were prepared by mounting grains in a steel cup. An acrylic plate with a microhole of 1470 µm diameter per 1860 µm depth was used to mount aliquots with similar volume and mass; each coarse-grained (sand) aliquot comprised approximately of 150 to 200 sand grains, as observed under the microscope, with average mass of 8.1 ± 0.9 mg (n=60). For the suspended silt samples, aliquots were prepared by evaporating four drops of

suspended sediment water solution over aluminum discs. Four fine-grained aliquots were measured per silt sample. X-ray fluorescence (XRF) measurements were used to determine the concentrations of Na, Ca, K and Si in polymineral sand aliquots; these measurements were performed in the Center for Nuclear Technologies of the Technical University of Denmark, using a Risø TL/OSL DA-20 reader equipped with a XRF attachment. Combined XRF and luminescence measurements were carried out in samples from the Solimões (11), Negro (5), Madeira (6) and Amazon (2) Rivers. The results of the XRF and luminescence measurements were correlated to evaluate the use of luminescence signals as a proxy for the concentration of feldspar relative to quartz grains.

The luminescence procedures (Table 1) included the bleaching of aliquots (step 1) to eliminate residual natural luminescence signals. Afterwards, 10 Gy and 50 Gy beta doses were given to induce luminescence signals in sand and silt aliquots, respectively. A pre-heat at 190ºC for 10s was applied before luminescence measurements to eliminate unstable signals. Infrared (IR) stimulation for 300 s (step 4) measured feldspars signal in polymineral aliquots. This step served the purpose of screening any quartz aliquots that suffer from feldspar contamination; such aliquots were subsequently rejected from data analysis. OSL using blue light stimulation (BOSL) at 125ºC was measured in step 5; this OSL signal represents quartz in case of pure quartz aliquots and is dominated by quartz in the polymineral aliquots. Step 6 repeated the OSL measurement to determine the background underlying the OSL obtained in step 5. The integral of the first 1s minus the last ten seconds of OSL emission from step 5 was used to estimate the intensity of the fast component ($BOSL_F$) dominated signal from quartz aliquots (Choi et al., 2006; Jain et al., 2003). A quartz OSL sensitivity ratio was obtained by dividing $BOSL_F$ from step 5 and the total OSL signal ($BOSL_T$) obtained from step 6. This ratio represents the relative intensity of the fast component compared to the slow and medium components and also normalizes for the dispersion in sensitivity estimates due to differences in the number of light emitting grains from aliquot to aliquot within the same sample. The signal from the feldspar fraction ($IRSL_I$) of the polymineral aliquots was estimated through the integration of the first 1.2 s of IRSL emission in step 4, minus the corresponding average intensity in the last ten

seconds. The $IRSL_I$ signal represents only the initial luminescence emission from feldspar grains and should not be confused with the fast OSL component. The $IRSL_I/BOSL_F$ (Step 4/Step 5) ratio was used as an index measuring the relative concentration of feldspar with respect to quartz; note that this is only an approximate index since $BOSL_F$ has also contribution from feldspar grains because of incomplete resetting of feldspar OSL by IR exposure at 125 °C (Jain and Singhvi, 2001). Furthermore, not all quartz grains may be emitting OSL (Duller, 2008).

Step	Procedure
1	Blue LEDs stimulation at 125°C for 100 s
2	Beta radiation dose of 10 Gy (sand) or 50 Gy (silt)
3	Pre-heat at 190°C for 10 s
4	Infrared stimulation at 60°C for 300 s
5	Blue LEDs stimulation at 125°C for 100 s
6	Blue LEDs stimulation at 125°C for 100 s

Table 1. The sequence of procedures used to measure luminescence sensitivity of sand and silt aliquots.

3.3. Fe and K concentrations in suspended sediments

Fe and K data measured in suspended sediments were used as a proxy for the provenance of sediments in the Amazon River basin. The concentrations of Fe and K are related to the intensity of chemical weathering (Govin et al., 2012) in sediment source areas and discriminate between sediments derived from Amazon Andean and Amazon lowland shield rivers (Govin et al. 2014). Fe and K in suspended sediments were measured using inductively coupled plasma-optical emission spectrometer (ICP-OES, Agilent 720) in the Marum-Center for Marine Environmental Sciences of the University of Bremen. Digestion of suspended material was performed with a microwave system (MLS, 1200 MEGA). For this purpose, 7 ml HNO_3 (65%), 0.5 ml HF (40%), 0.5 ml HCl (30%), and 0.5 ml MilliQ was added to about 50 mg sample material (filter + suspended material) previously placed into Teflon liners. All acids were of suprapure quality. See Zhang et al. (2017) for a detailed description of Fe/K data.

4. Results

Luminescence sensitivity results (Tables 2 and 3 and Supplementary Table S1) show that riverbed sands and suspended silt of rivers with Andean headwaters like the Solimões, Içá, Japurá and Madeira Rivers show lower sensitivity ($BOSL_F$) compared to sand and silt from shield rivers like the Tapajós and Xingu Rivers. Sediments from the Madeira River have higher sensitivity than sediments from the Solimões River. Sand grains from the Negro River have intermediate sensitivity (Figure 2). The Tapajós and Xingu Rivers stand out by the presence of sand grains with higher variability of sensitivity across samples.

Results from pure quartz aliquots (Table 3 and Figure 2) confirmed the higher sensitivity of quartz from shield rivers (Xingu and Tapajós). The exception is the similarity between the sensitivity of quartz from the Negro and Madeira Rivers. Suspended silt and riverbed sands show similar patterns of sensitivity variation among rivers. The variations in the luminescence sensitivity are significantly larger than the 11% random uncertainty in aliquot mass (8.1 ± 0.9 mg). This confirms that that our aliquot preparation approach combined with luminescence signal normalization does not induce any systematic variations in measured sensitivity of the studied sand samples.

River	N	$\%BOSL_F/BOSL_T$		$IRSL_I/BOSL_F$	
		Average	Std. dev.	Average	Std. dev.
Içá	5	9.20	2.64	112.75	29.56
Jutaí	3	23.14	0.84	48.60	22.39
Juruá	5	15.51	1.52	64.52	2.56
Japurá	5	7.89	0.61	112.81	34.93
Tefé	1	10.67	-	104.03	-
Coari	1	11.79	-	82.18	-
Purus	5	14.56	1.90	66.94	9.03
Solimões	10	7.57	0.64	157.44	22.66
Negro	7	19.6	13.08	72.79	17.34
Madeira	5	10.17	1.37	113.03	8.66
Tapajós	4	29.38	16.15	43.80	15.21
Xingu	5	25.16	12.23	51.47	20.30
Amazon	14	9.89	1.17	126.36	23.91

Table 2 – Summary of luminescence sensitivity results for suspended sediment samples (silt grain size). N is the number of samples per river.

River	Polymineral aliquots (quartz+feldspar)					Pure quartz aliquots		
	N	$\%BOSL_F/BOSL_T$		$IRSL_I/BOSL_F$		$\%BOSL_F/BOSL_T$		
		Average	Std. dev.	Average	Std. dev.	N	Average	Std. dev.
Solimões	21	4.27	0.62	83.46	16.22	6	15.37	5.04
Negro	9	14.53	6.82	33.40	22.70	3	25.26	14.86
Madeira	16	6.47	2.33	66.28	26.46	6	31.65	10.99
Tapajós	13	57.41	12.08	2.56	3.19	4	65.73	5.73
Xingu	9	42.08	13.59	2.16	1.68	6	56.26	7.25
Amazon	25	5.76	5.01	81.12	23.74	3	19.22	1.81

Table 3 – Summary of luminescence sensitivity results for riverbed sediment samples (sand grain size). N is the number of samples per river.

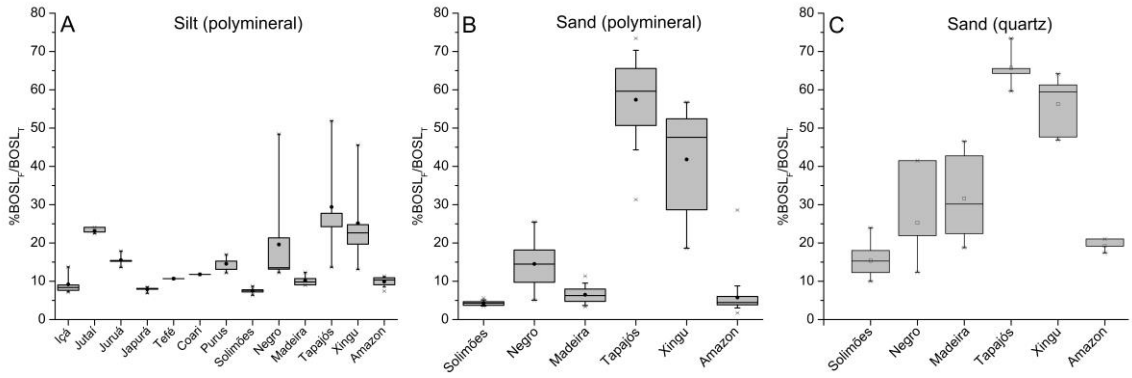

Figure 2 – Luminescence sensitivity of samples from the Amazon River and its major tributaries. Data from polymineral suspended silt (A), polymineral riverbed sand (B), and pure quartz riverbed sand (C) are organized from upstream (left) to donwstream (right) tributaries of the Solimões-Amazon main stem.

The ratio $BOSL_F/BOSL_T$ represents the relative intensity of the quartz fast OSL component compared to the slowly bleaching component(s). The slow and medium component(s) in the polymineral aliquots contains an additional contribution from the slowly bleaching feldspar signal than in the pure quartz aliquots. Similarly, the intensity of IRSL from an aliquot is both a function of the sensitivity and proportion of feldspar in that aliquot. It is expected that for the given sensitivity of quartz, the $BOSL_F/BOSL_T$ ratio in polymineral aliquots should decrease with an increase in the feldspar concentration both due to the reduced quantity of quartz (dilution effect), as well as an increase in the $BOSL_T$ due to feldspar contribution (note that these are both linear effects). This is exactly what we observe in the polymineral data; both suspended silt and riverbed sands show a trend of increasing $BOSL_F$ sensitivity with

decreasing $IRSL_I$ sensitivity and feldspar content (Figure 3). Note that the near-zero value on the x axis indicates the pure quartz fractions; the spread in y values here is thus the true variation in the sensitivity of the quartz OSL component across samples.

The $IRSL_I/BOSL_F$ ratio is positively correlated with the concentrations of Na and Ca, but a negligible correlation (R^2=0.02) was observed between $IRSL_I/BOSL_F$ ratio and K (Figure 4 and Supplementary Table S2). This suggests that the IRSL intensity variation is controlled by Na-Ca feldspar concentration. The K content does not show a clear correlation due to the presence of a few high K bearing aliquots with below average sensitivity. The likely explanation for this result is that K may be contained in non-feldspar minerals such as biotite and muscovite. In summary, these results point out that the relative $BOSL_F$ sensitivity is decreasing with an increase in the feldspar content, thus suggesting that the amount of feldspar grains is the dominant source affecting the $BOSL_F$ sensitivity in the polymineral aliquots.

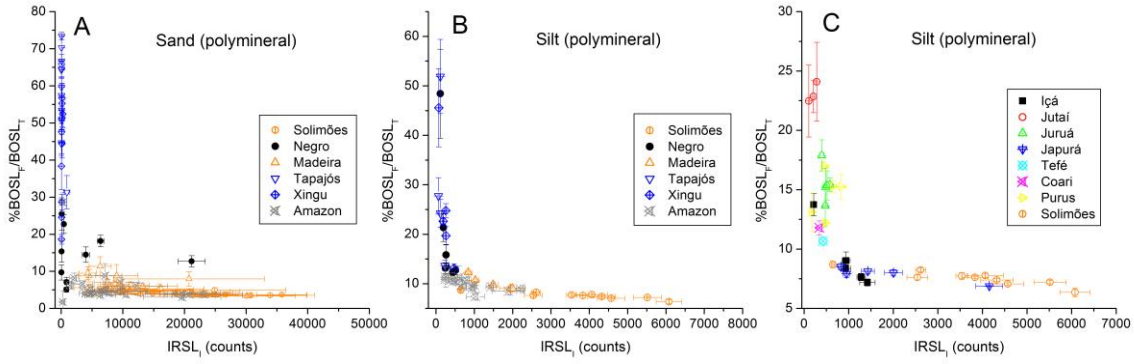

Figure 3 – Variation of $BOSL_F$ and $IRSL_I$ luminescence sensitivities in polymineral aliquots of riverbed sand (A) and suspended silt (B) of the major tributaries of the Amazon River. Luminescence sensitivities of suspended silt from tributaries of the Solimões River are shown in C. Samples named as "Solimões" correspond to sediments from the Solimões River main stem. Data are organized from upstream (left) to donwstream (right) tributaries of the Solimões-Amazon main stem.

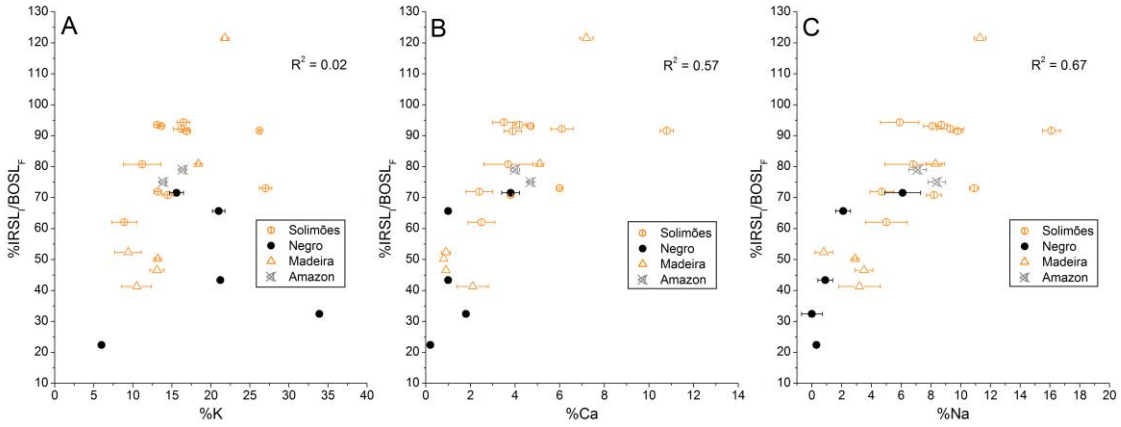

Figure 4 – Variation of potassium (A), calcium (B) and sodium (C) contents compared to the $IRSL_I/BOSL_F$ ratio measured in polymineral sand aliquots of the Solimões (11), Negro (5), Madeira (6) and Amazon (2) Rivers.

Sediments from the Solimões, Madeira and Amazon Rivers, which have larger catchments, requiring longer distances of sediment transport from headwaters to the sampling sites, have quartz grains with lower sensitivity (Figure 5 and Table 3). Also, a systematic trend of increase in quartz sensitivity ($BOSL_F$) with distance from the sediment source areas is not observed along the Solimões-Amazon River main stem (Figure 5 and Supplementary Table S3). The Fe/K ratio has been used as a proxy to differentiate between sediments of Andean and lowland shield tributaries of the Amazon River (Govin et al. 2014). In the studied samples, the Solimões, Madeira and Amazon Rivers show suspended sediments enriched in K (low Fe/K), with little variation between the low and high water level periods (Figure 6). The higher concentration of K in sediments of these Rivers fits with their higher $IRSL_I$ signal, confirming higher feldspar concentration in sediments from these rivers. Suspended sediments transported by the Negro, Tapajós and Xingu Rivers show higher Fe/K values, with significant increase in Fe concentration during the high water level period, when rainfall increases the input of sediments derived from the erosion of heavy weathered soils. Lateritic soil profiles that cover most of the upstream shield areas are enriched in Fe oxides and hydroxides, which are transported to the river channels during the rainy season.

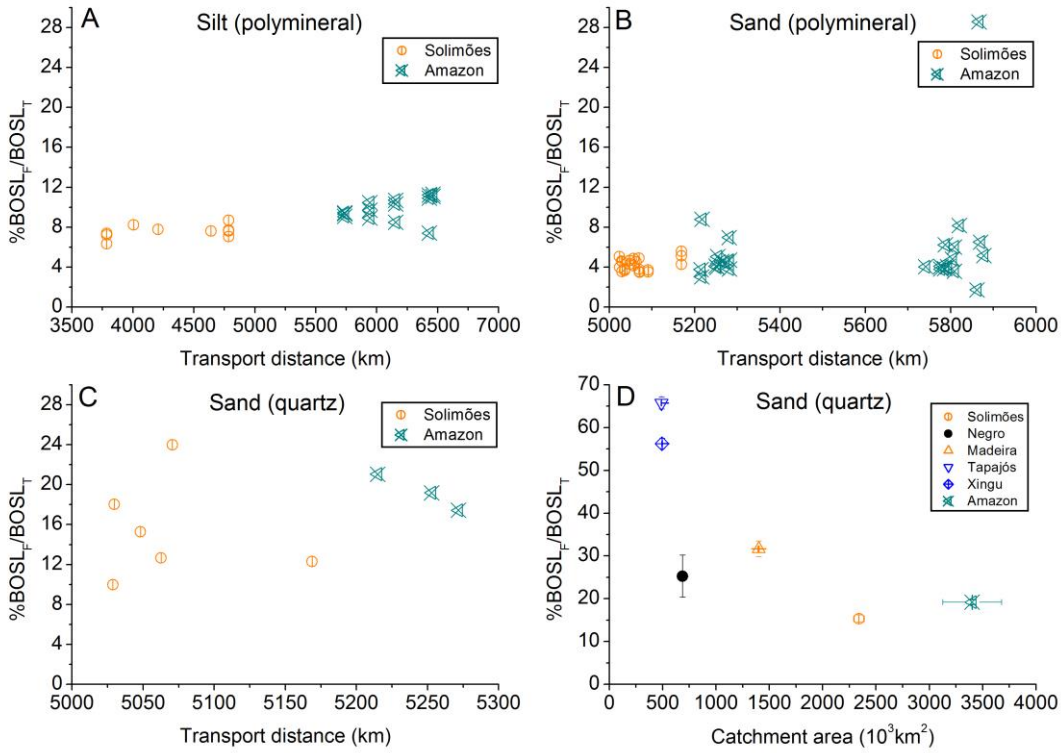

Figure 5 – Variation in luminescence sensitivities of polymineral silt (A), polymineral sand (B) and pure quartz sand (C) along the Solimões-Amazon River main stem. A comparison between the sensitivity of quartz and the catchment area upstream the sampling sites are shown in D. Each river is represented by the average and standard deviation (error bars) values of quartz sensitivity and catchment area.

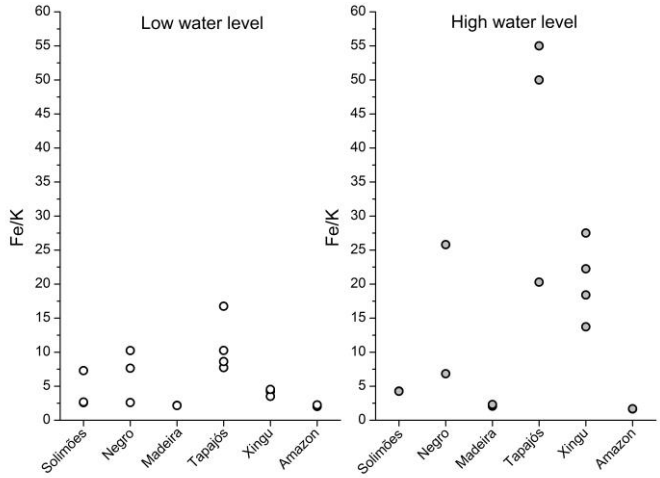

Figure 6 – Fe/K ratio in suspended sediments sampled during the low (A) and high (B) water level periods. Number of samples: Solimões high=3, low=3; Madeira high=3, low=3; Negro high=3, low=2; Tapajós high=3, low=4; Xingu high=4, low=4.

The IRSL signal from the polymineral aliquots shows a positive correlation with denudation rate determined through ^{10}Be concentrations (Wittmann et al., 2010) in sediments from the Amazon rivers (Figure 7). This correlation suggests that for areas with high denudation rates there is relatively less time available for chemical weathering of feldspar; thus, the resulting fine sand fraction has a higher feldspar to quartz ratio. However, interestingly the $BOSL_F$ signal from pure quartz aliquots correlates negatively with denudation rates; this is a new observation, which suggests that landscape denudation may play an important role in luminescence sensitization of quartz.

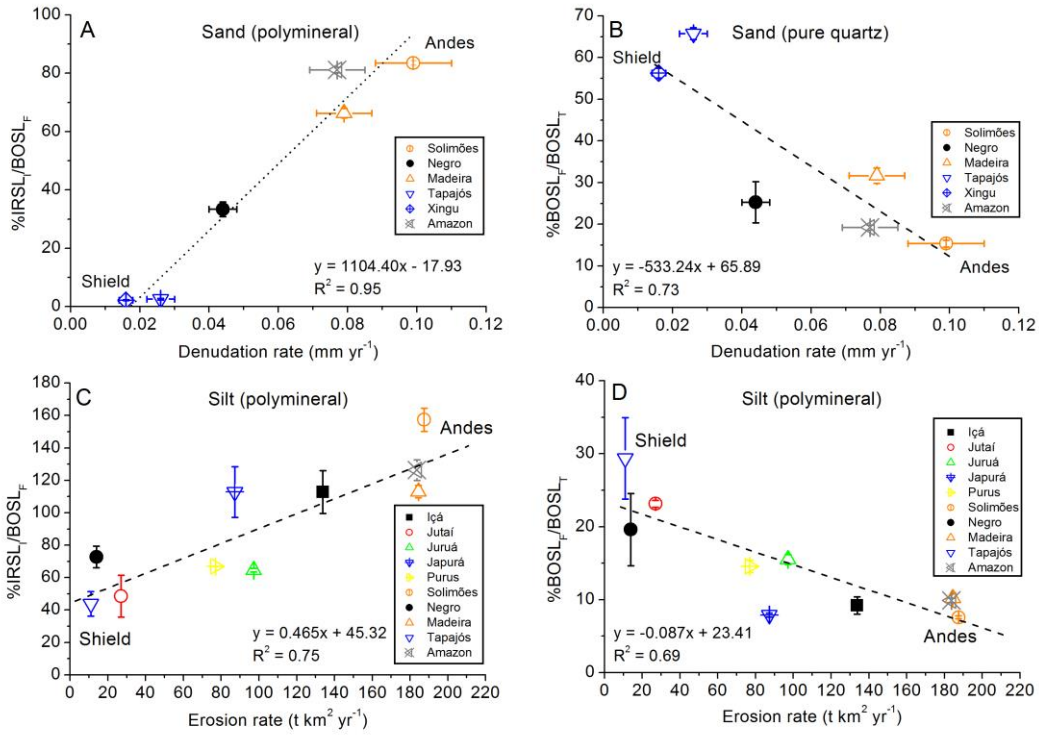

Figure 7 – Variation of luminescence signals of feldspar (A) and quartz (B) from riverbed sands in terms of denudation rates derived from ^{10}Be concentrations measured in quartz (125-250 μm). Feldspar ($\%IRSL_I/BOSL_F$) and quartz ($\%BOSL_F/BOSL_T$) signals respectively measured in polymineral and pure quartz aliquots from fine sand. Denudation rates data compiled from Wittmann et al. (2010). In Wittmann et al. (2010), the samples from the Tapajós and Xingu Rivers represent sediments from headlands. Samples from Negro, Madeira and Solimões Rivers are from lower reaches near the sites sampled in this study. Samples from

371 the Amazon River represent sediments from sectors downstream the Madeira River and
372 upstream the Tapajós River (Parintins and Óbidos). C and D show the ratios $\%IRSL_I/BOSL_F$
373 and $\%BOSL_F/BOSL_T$ measured in polymineral aliquots of suspended silt in terms of erosion
374 rates calculated through sediment gauging stations. Erosion rates data compiled from Bouchez
375 et al. (2014).
376
377 **5. Discussion**
378 **5.1. Sensitization of quartz OSL in nature**
379 OSL sensitivity is a fundamental property of quartz for its use as a luminescence
380 geochronometer. The relationship between OSL and the radiation dose accumulated since the
381 last daylight exposure of quartz grains allows estimation of the sediment burial age. There have
382 been numerous studies in the past to understand OSL characteristics of quartz for its robust
383 application in geochronometry. However, most of these studies have focused on laboratory-
384 induced changes in the quartz OSL using a combination of heat, light or ionizing radiation
385 (Wintle and Adamiec, 2017), and the drivers that induce quartz OSL sensitization in nature are
386 still poorly understood.
387 Quartz extracted from different types of igneous and metamorphic rocks has a
388 relatively low sensitivity (Chithambo et al., 2007; Guralnik et al., 2015) compared to quartz
389 from sediments (Sawakuchi et al., 2011). Heating was the first factor recognized to increase the
390 luminescence sensitivity of quartz (Bøtter-Jensen et al., 1995). However, significant
391 sensitization of different OSL components of quartz only occurs after heating to temperatures
392 above 300ºC (Jain et al., 2003), which is not likely in surface sedimentary environments.
393 Interestingly, the luminescence sensitivity of quartz grains from sediments can vary by several
394 orders of magnitude (Pietsch et al., 2008). These observations suggest that the sensitization of
395 quartz occurs somewhere between source to sink in sedimentary environments.
396 Pietsch et al. (2008) and Gliganic et al. (2017) observed a positive correlation between
397 the OSL sensitivity of quartz and downstream distance of sediment transport along Australian
398 rivers, proposing that sensitization occurs due to cycles of irradiation under burial and solar

399 exposure during sediment transport. However, the increase in OSL sensitivity with the distance
400 of sediment transport is not confirmed by our new data from the Amazon rivers. On the
401 contrary, lower sensitivity quartz occurs in the Solimões, Madeira and Amazon Rivers, which
402 have longer sediment transport pathways and larger catchment areas (Figure 5). Thus,
403 luminescence characteristics inherited from sediment source rocks or other surface processes
404 can drive the sensitization of quartz in the Amazon fluvial system.

405 Quartz from sediments deposited around mountain ranges like the New Zealand Alps
406 (Preusser et al., 2006), European Alps (Klasen et al., 2007), Scottish Highlands (Lukas et al.,
407 2007), Andes (Steffen et al., 2009) and Himalayas (Jaiswal et al., 2008) usually has very low
408 luminescence sensitivity. On the other hand, regions lacking young high relief mountain ranges
409 like southeastern Australia (Fitzsimmons et al., 2010) and northeastern and southestern Brazil
410 (Guedes et al., 2011) have widespread occurrence of sediments with high sensitivity quartz
411 grains suitable for luminescence dating. This geographical pattern implies that mountain
412 building and rates of uplift and erosion may play an important role in the sensitization of quartz
413 in nature. In the studied rivers, quartz with the lowest OSL sensitivity is provided by the
414 Solimões River (Figures 1 and 2, Tables 2 and 3), where most of its sediments are supplied by
415 the Andes mountain belt (Gibbs, 1967; Govin et al., 2014). Quartz with higher sensitivity
416 occurs in the Tapajós and Xingu Rivers, which exclusively drain stable cratonic areas of the
417 Central Brazil shield. The Madeira and Negro Rivers have quartz with intermediate sensitivity,
418 indicating a mixture of sediments from Andean and shield sources. This is in agreement with
419 the area drained by these rivers. Despite its Andean headwaters, the middle and lower Madeira
420 River receive sediments from tributaries running over the Central Brazil shield. On the other
421 hand, the Negro River mostly drains the Guiana shield, but has lowland tributaries draining
422 Quaternary terraces of the Japurá and Solimões Rivers, whose sediments are provided mainly
423 by Andean sources.

424 The sediment source rocks in Andes, Central Brazil and Guianas are very diverse and
425 include many types of igneous, sedimentary and metamorphic rocks (Jaillard et al., 2000;
426 Tassinari et al., 2000; Rossetti et al., 2005). The headwaters of the Madeira and Solimões Rivers

427 are located in the Eastern Cordillera of the Bolivian and Peruvian Andes, an area with
428 widespread occurrence of Mesozoic and Neogene volcanic and metasedimentary rocks.
429 However, most of the Andean drainages flowing to the lowland Amazon run over sediments of
430 the subandean zone and of the eastern Andean lowlands (Jailard et al., 2000). The shield areas
431 in Central Brazil and Guianas are dominated by Pre-Cambrian metamorphic and intrusive
432 igneous rocks. Upstream areas of the Xingu and Tapajós Rivers also include Paleozoic and
433 Mesozoic sedimentary rocks that overlay the metamorphic and igneous rocks of the southern
434 portion of the Central Brazil shield. Andean and shield areas also have contrasting denudation
435 rates as indicated by fluvial sediment flux and total dissolved solids data (Bouchez et al., 2014;
436 Moquet et al., 2016) and cosmogenic nuclide data (Wittman and Blanckendburg, 2009;
437 Wittmann et al., 2009; 2010). Denudation rates in river catchments from Andes (0.5 $mm.yr^{-1}$)
438 and shield Amazon (0.01 $mm.yr^{-1}$) catchments differ by one order of magnitude (Wittmann et
439 al., 2010). The different geological context between Andes and shield areas define two end-
440 member sediment compositions that are sourced to the Amazon River basin (Basu et al., 1990;
441 Viers et al., 2008). The higher feldspar content in Andean sediments, as indicated by the higher
442 $IRSL_I/BOSL_F$ ratio in sediments from the Solimões River (Figure 3, Tables 2 and 3), further
443 confirms that lower sensitivity quartz is derived from rocks located in catchments under higher
444 denudation rates. In this case, higher denudation rates in Andes are linked to fast erosion of
445 soils, which allows short time for chemical weathering and, thus, favors the preservation of
446 feldspar grains in river sediments. On the other hand, geological settings under lower
447 denudation rates (e.g. Tapajós and Xingu Rivers) promote longer weathering time and thereby
448 reduced feldspar input (due to weathering), and high sensitivity quartz. Also, the Solimões,
449 Negro and Madeira Rivers flow through major Quaternary and Neogene sediment accumulation
450 areas in lowland Amazonia (Rossetti et al., 2005) while the Tapajós and Xingu Rivers comprise
451 bedrock incised channels with low accommodation space and high sediment bypass. On
452 average, it is expected that sediment quartz grains have a higher near-surface residence time in
453 low relief, slowly eroding catchments due to low accommodation space (Jain et al., 2004)
454 compared to quartz grains derived from rocks in high relief, fast eroding catchments. It is

plausible that the average residence time of quartz grains in soil profiles and weathering processes in the surface environment may play an important role for luminescence sensitization of quartz. The sensitivities of suspended silt (polymineral aliquots) and riverbed sand (pure quartz aliquots) show minor variation along transport distances of respectively 2750 km and 250 km in the Solimões-Amazon River main stem (Figure 5). This may suggest that sediment transport has minimal influence on the luminescence sensitization of sediments in the Amazon basin.

The inverse relationship between denudation rates and quartz OSL sensitivity (Figure 7B) allows us to propose that the exhumation and weathering history of the source rocks have a significant influence on the OSL sensitization of quartz. In addition to the surface residence time, other factors such as uplift rate and age of source rocks may also influence quartz sensitivity. For example, sensitization may be related to the thermal (cooling) history of source rocks; lower uplift rates imply proportionately longer storage time under higher subsurface temperatures. The age of source rocks can also contribute to sensitization since older rocks will promote a higher absorbed radiation dose in quartz crystals before they become sediment grains. The accumulated dose in quartz crystals provided by Cenozoic or Pre-Cambrian igneous and metamorphic source rocks can differ in several orders of magnitude. Quartz crystals within Proterozoic granites (810-580 Ma) from Brazilian shield areas were exposed to radiation doses about 4.1-5.7 MGy, assuming dose rates of 7 Gy/ka (gamma and beta) calculated through average concentrations of U, Th and K obtained for granite plutons from southeastern Brazil (Alves et al., 2016). The combination of higher accumulated dose and longer heating of source rocks from Pre-Cambrian shield areas under slow uplift rates resembles a natural pre-dose and accumulated thermal sensitization effects (Bailey, 2001).

Finally, the sensitization of quartz may be related to chemical weathering processes. Our data suggest that more sensitive quartz comes from source rocks exposed to longer duration of chemical weathering (because of lower denudation rates). According to Sharma et al. (2017) quartz samples with higher water content have lower OSL sensitivity, implying that water-related defects increase the efficiency of non-radiative recombination centers and favor

luminescence quenching. However, it is not clear how water molecules are driven out of quartz in areas of low denudation (high weathering) rates. This effect must only be important once the rock enters the active weathering zone. Another hypothesis to link denudation and weathering processes and luminescence sensitization is that the fragmentation of larger quartz crystals during weathering increases the capacity of the alpha and beta radiation in promoting physical damage in quartz. Considering that quartz has a negligible amount of radionuclides, quartz crystal fragmentation and production of smaller quartz grains increase the interaction between grains and the external radionuclide-derived alpha and beta radiation. Additionaly, the interaction between the cosmic radiation and quartz increases when source rocks reach shallower depths. Thus, the effect of the ionizing radiation on quartz grains possibly produces deffects related to luminescence processes. Further studies are necessary to evaluate if the sensitization of quartz in the Amazon fluvial system is related to a relative decrease of non-radiative (K-centers) recombination centers (Bailey, 2001) or to changes in electron traps associated with the OSL fast component.

5.2. Sources of suspended and riverbed sediments in the Amazon River basin

Despite the incomplete understanding about natural sensitization of quartz in terms of its electron-hole trapping system, the luminescence signals related to quartz ($BOSL_F$) and feldspar ($IRSL_I$) clearly discriminate between Andean and shield sediments (Figure 3, Tables 2 and 3). Thus, luminescence signals of quartz and feldspar are useful proxies to track the relative contribution of Andean and shield areas to the suspended and riverbed sediments transported by the Amazon River. The $BOSL_F/BOSL_T$ ratio (Figure 2) indicates that the Madeira River is the major source of silt to the Amazon River, which is confirmed by Fe/K data (Figure 6), in accordance with other studies showing that Andean rivers dominate the suspended sediment load delivered by the Amazon River to the Atlantic Ocean (Govin et al., 2014; Zhang et al., 2017). Riverbed sands show a different provenance pattern, with higher contribution of sands from the Solimões River (Figures 2 and 3). The $BOSL_F/BOSL_T$ ratio measured in pure quartz aliquots also indicates significant contribution of cratonic sands to the

Madeira River, pointing to a high decoupling between the sources of silt (Andean) and sand (Andean-Shield). The decoupling between catchment area and sediment supply is also observed for the Solimões River. The Solimões River sediments have low sensitivity, which is similar to that presented by the Içá and Japurá Rivers. On the other hand, sediments from lowland tributaries (Jutaí, Juruá, Tefé, Coari and Purus River) of the Solimões River have higher sensitivity, suggesting a mixture of sediments from Andean and shield sources (Figures 2 and 3). The $BOSL_F/BOSL_T$ ratio also differentiates sediments supplied by shield rivers (Negro, Xingu and Tapajós), which are similar regarding their major elemental composition (Govin et al., 2014; Zhang et al., 2017).

Paleoenvironmental changes in the Amazon River basin have been reconstructed through proxies based on inorganic geochemistry of suspended sediments deposited offshore the Amazon River mouth (Govin et al., 2014). However, suspended sediments of the Andean rivers dominate the inorganic geochemical signals measured in sediments of the Amazon River, potentially hindering the recognition of paleoenvironmental changes in shield and lowland areas. Shield rivers have a low suspended load (Sioli, 1985), but represent a significant portion of the Amazon River basin, including the Negro River, its second largest tributary (Figure 1). Our study suggests that quartz OSL sensitivity may be useful to reconstruct paleoenvironmental changes in the Amazon River basin, including these underrepresented areas because the clear distinction between OSL sensitivity of quartz from shield rivers compared to that from the Andean rivers. The high abundance and high stability of quartz to weathering and diagenetic processes combined with fast and easy-to-make luminescence measurements are great advantages of the luminescence techniques to constrain changes in sediments provenance in the Amazon River basin and potentially in other large river contexts.

6. Conclusions

Optically stimulated luminescence signals fingerprint the sources of quartz and feldspar in suspended and riverbed sediments of Amazon rivers. The intensity of the IRSL signal indicates the relative concentration of feldspar in sediments. The correlation observed

between quartz OSL sensitivity and denudation rate in the source area suggests that near-surface residence time of quartz grains and possible thermal/irradiation history may play an important role in sensitization of quartz in nature. This correlation explored for the first time in this study highlights the use of quartz OSL sensitivity as a complementary proxy for sediment sources and denudation rate estimates. Additionaly, luminescence signals measured in riverbed sand and suspended silt arise from the same components (quartz and feldspar), avoiding the inevitable grain size bias in provenance analysis caused by the large difference between the traction and the suspended load of the Andean rivers and the shield rivers. The qualitatively and quantitatively relationship between quartz OSL sensitivity and denudation rates in sediment source areas is promising to develop methods for studying landscape evolution. Finally, we show that in the context of the Amazon fluvial system both the IRSL intensity (a proxy for quartz to feldspar ratio) as well as the quartz OSL sensitivity can be tied to the provenance. Thus, a quantitative change in these proxies measured in the stratigraphic record may be linked to past provenance scenarios and variation in denudation rates, which can track precipitation changes and drainage configuration in sediment source areas.

Acknowledgments

We are grateful to Jean-Sébastien Moquet and two anonymous Reviewers for the remarkable suggestions and comments that greatly contribute to improve this manuscript. This research was funded by São Paulo Research Foundation under the project “Provenance and storage of sediments in Amazon rivers” (FAPESP 2011/06609-1) and project “Structure and evolution of the Amazonian biota and its environment: an integrative approach”, a collaborative Dimensions of Biodiversity-BIOTA grant supported by FAPESP (grant #2012/50260-6), National Science Foundation (NSF DEB 1241066), and National Aeronautics and Space Administration (NASA). The Brazilian National Council for Scientific and Technological Development supports AOS (CNPq grant 3009223/2014-8), CMC (CNPq grants 302607/2016-1 and 422255/2016-5) and CHG (CNPq grant 307647/2015-3). FNP was supported by post-doctorate fellowships from FAPESP (grants 2014/23334-4 and 2016/09293-9).

567

568 **References**

569 Alves, A., Janasi, V.A., Campos Neto, M.C., 2016. Sources of granite magmatism in the Embu
570 Terrane (Ribeira Belt, Brazil): Neoproterozoic crust recycling constrained by elemental and
571 isotope (Sr-Nd-Pb) geochemistry. Journal of South American Earth Sciences 68, 205-223.

572

573 Bailey, R.M., 2001. Towards a general kinetic model for optically and thermally stimulated
574 luminescence of quartz. Radiation Measurements 33, 17-45.

575

576 Basu, A.R., Sharma, M., DeCelles, P.G., 1990. Nd, Sr-isotopic provenance and trace element
577 geochemistry of Amazonian foreland basin fluvial sands, Bolivia and Peru: implications for
578 ensialic Andean orogeny. Earth and Planetary Science Letters 100, 1-17.

579

580 Bøtter-Jensen, L., Agersnap Larsen, N., Mejdahl, V., Poolton, N.R.J., Morris, M.F., McKeever,
581 S.W.S., 1995. Luminescence sensitivity changes in quartz as a result of annealing. Radiation
582 Measurements 24(4), 535-541.

583

584 Bouchez, J., Gaillardet, J., France-Lanord, C., Maurice, L., Dutra-Maia, P., 2011. Grain size
585 control of river suspended sediment geochemistry: clues from Amazon River depth profiles.
586 Geochemistry, Geophysics, Geosystems 12, 1–24.

587

588 Bouchez, J., Gaillardet, J., Von Blanckenburg, F., 2014. Weathering intensity in lowland river
589 basins: from the Andes to the Amazon mouth. Procedia Earth and Planetary Science 10, 280-
590 286.

591

592 Chithambo, M.L., Preusser, F., Ramseyer, K., Ogundare, F.O., 2007. Time-resolved
593 luminescence of low sensitivity quartz from crystalline rocks. Radiation Measurements 42(2),
594 205-212.
595
596 Choi, J.H., Duller, G.A.T., Wintle, A.G., Cheong, C.-S., 2006. Luminescence characteristics of
597 quartz from the Southern Kenyan Rift Valley: dose estimation using LM-OSL SAR. Radiation
598 Measurements 41, 847-854.
599
600 Dobson, D. M., Dickens, G. R., Rea, D. K., 2001. Terrigenous sediment on Ceara Rise: a
601 Cenozoic record of South American orogeny and erosion. Palaeogeography,
602 Palaeoclimatology, Palaeoecology 165(3), 215-229.
603
604 Duller, G. A., 2008. Single-grain optical dating of Quaternary sediments: why aliquot size
605 matters in luminescence dating. Boreas 37(4), 589-612.
606
607 Espinoza Villar, J.C., Ronchail, J., Guyot, J.L., Cochonneau, G., Filizola, N., Lavado, W., De
608 Oliveira, E., Pombosa, R., Vauchel, P., 2009. Spatio-temporal rainfall variability in the Amazon
609 basin countries (Brazil, Peru, Bolivia, Colombia, and Ecuador). International Journal of
610 Climatology 29(11), 1574-1594.
611
612 Filizola, N., Guyot, J.L., 2009. Suspended sediment yields in the Amazon basin: an assessment
613 using the Brazilian national data set. Hydrological Processes 23, 3207-3215.
614
615 Fitzsimmons, K.E., Rhodes, E.J., Barrows, T.T., 2010. OSL dating of southeast Australian
616 quartz: a preliminary assessment of the luminescence characteristics and behaviour. Quaternary
617 Geochronology 5, 91-95.
618

Gibbs, R.J., 1967. The Geochemistry of the Amazon River System: Part I. The Factors that Control the Salinity and the Composition and Concentration of the Suspended Solids. Geological Society of America Bulletin 78(10), 1203-1232.

Gliganic, L.A., Cohen, T.J., Meyer, M., Molenaar, A., 2017. Variations in luminescence properties of quartz and feldspar from modern fluvial sediments in three rivers. Quaternary Geochronology 41, 70-82.

Govin, A., Chiessi, C. M., Zabel, M., Sawakuchi, A. O., Heslop, D., Hörner, T., Zhang, Y., Mulitza, S., 2014. Terrigenous input off northern South America driven by changes in Amazonian climate and the North Brazil Current retroflection during the last 250 ka. Climate of the Past 10(2), 843-862.

Govin, A., Holzwarth, U., Heslop, D., Ford Keeling, L., Zabel, M., Mulitza, S., Collins, J. A., Chiessi, C. M., 2012. Distribution of major elements in Atlantic surface sediments (36° N–49° S): Imprint of terrigenous input and continental weathering. Geochemistry Geophysics Geosystems 13, Q01013, doi:10.1029/2011gc003785.

Guedes C.C.F., Giannini P.C.F., Sawakuchi A.O., DeWitt R., Nascimento Jr. D.R., Aguiar V.A.P., Rossi M.G., 2011. Determination of controls on Holocene barrier progradation through application of OSL dating: the Ilha Comprida Barrier example, Southeastern Brazil. Marine Geology 285,11-16.

Guralnik, B., Ankjærgaard, Jain, M., Murray, A.S., Müller, A., Wälle, M., Lowick, S.E., Preusser, F., Rhodes, E.J., Wu, T.-S., Herman, F., 2015. OSL-thermochronometry using bedrock quartz: A note of caution. Quaternary Geochronology 25, 37-48.

Guyot, J.L., Jouanneau, J.M., Soares, L., Boaventura, G.R., Maillet, N., Lagane, C., 2007. Clay mineral composition of river sediments in the Amazon Basin. Catena 71, 340–356.

Jaillard E., Hérail G., Monfret T., Díaz-Martínez E., Baby P., Lavenu A., Dumont J.F., 2000. Tectonic evolution of the Andes of Ecuador, Peru, Bolivia and northernmost Chile. *In:* Cordani, U.G., Thomaz-Filho, A., Campos, D.A. (Eds.) Tectonic Evolution of South America. Acad. Bras. Cienc. Spec. Publ. 31st Int. Geol. Cong., pp. 41-95.

Jain, M., Singhvi, A. K., 2001. Limits to depletion of blue-green light stimulated luminescence in feldspars: implications for quartz dating. Radiation Measurements 33(6), 883-892.

Jain, M., Murray, A.S., Bøtter-Jensen, L., 2003. Characterisation of blue-light stimulated luminescence components in different quartz samples: implications for dose measurement. Radiation Measurements 37, 441-449.

Jain, M., Murray, A.S., Bøtter-Jensen, L., 2004. Optically stimulated luminescence dating: how significant is incomplete light exposure in fluvial environments? Quaternaire 15(1-2), 143-157.

Jaiswal, M.K., Srivastava, P., Tripathi, J.K., Islam, R., 2008. Feasibility of the SAR technique on quartz sand of terraces of NW Himalaya: a case study from Devprayag. Geochronometria 31, 45-52.

Juyal, N., Pant, R.K., Bhushan, R., Jain, M., Saini, N.K., Yadava, M.G., Singhvi, A.K., 2009. Reconstruction of Last Glacial to early Holocene monsoon variability from relict lake sediments of the Higher Central Himalaya, Uttrakhand, India. Journal of Asian Earth Sciences 34(3), 437-449.

674 Klasen, N., Fiebig, M., Preusser, F., Reiner, J.M., Radtke, U., 2007. Luminescence dating of
675 proglacial sediments from the Eastern Alps. Quaternary International 164-165, 21-32.
676
677 Latrubesse, E.M., Stevaux J.C., Sinha R., 2005. Tropical Rivers. Geomorphology 70, 187-206.
678
679 Lü, T.Y., Sun, J., Li, S-H, Gong, Z., Xue, L., 2014. Vertical variations of luminescence
680 sensitivity of quartz grains from loess/paleosol of Luochuan section in the central Chinese
681 Loess Plateau since the last interglacial. Quaternary Geochronology 22, 107-115.
682
683 Lukas, S., Spencer, J.Q.G., Robinson, R.A.J., Benn, D.I., 2007. Problems associated with
684 luminescence dating of Late Quaternary glacial sediments in the NW Scottish Highlands.
685 Quaternary Geochronology 1-4, 243-248.
686
687 McClain, M.E., Naiman, R.J., 2008. Andean influences on the biogeochemistry and ecology of
688 the Amazon River. BioScience 58(4), 325-338.
689
690 Meade, R.H., 1994. Suspended sediments of the modern Amazon and Orinoco rivers.
691 Quaternary International 21, 29-39.
692
693 Moquet, J-S., Guyot, J-L., Crave, A., Viers, J., Filizola, N. et al. 2016. Amazon River dissolved
694 load: temporal dynamics and annual budget from the Andes to the ocean. Earth Science and
695 Pollution Research 23(12), 11405-11429.
696
697 Morton, A.C., Hallsworth, C.R., 1999. Processes controlling the composition of heavy
698 mineral assemblages in sandstones. Sedimentary Geology 124(1-4), 3–29.
699

Nittrouer, C.A., Kuehl, S.A., Sternberg, R.W., Figueiredo Jr., A.G., Faria, L.E.C., 1995. An introduction to the geological significance of sediment transport and accumulation on the Amazon continental shelf. Marine Geology 125(3-4), 177-192.

Pietsch, T.J., Olley, J.M., Nanson, G.C., 2008. Fluvial transport as a natural luminescence sensitiser of quartz. Quaternary Geochronology 3, 365-376.

Preusser, F., Ramseyer, K., Schlüchter, C., 2006. Characterization of low OSL intensity quartz from the New Zealand Alps. Radiation Measurements 41, 871-877.

Rossetti, D.F, Toledo, P.M., Góes A.M., 2005. New geological framework for Western Amazonia (Brazil) and implications for biogeography and evolution. Quaternary Research 63, 78–89.

Sawakuchi, A.O., Blair, M.W., DeWitt, R., Faleiros, F.M., Hyppolito, T.N., Guedes, C.C.F., 2011. Thermal history versus sedimentary history: OSL sensitivity of single quartz grains extracted from igneous and metamorphic rocks and sediments. Quaternary Geochronology 6, 261-272.

Sawakuchi, A.O., Guedes, C.C.F., DeWitt, R., Giannini, P.C.F., Blair, M.W., Nascimento Jr., D.R., Faleiros, F.M., 2012. Quartz OSL sensitivity as a proxy for storm activity on the southern Brazilian coast during the Late Holocene. Quaternary Geochronology 13, 92-102.

Sharma, S.K., Chawla, S., Sastry, MD., Gaonkar, M., Mane, S., Balaram, V., Singhvi, A.K., 2017. Understanding the reasons for variations in luminescence sensitivity of natural quartz using spectroscopic and chemical studies. Proceeding of the Indian National Science Academy, doi: 10.16943/ptinsa/2017/49024.

Silva, C.R., Peixinho, F.C., Monteiro, A., Pinto, E.J.A., Azambuja, A.M.S., Farias, J.A.M., Pickbrenner, K., Weschendelder, A.B., Santos, A.L.M.R., Marcuzzo, F.F.N., Costa, M.R., Nascimento, J.R.S., Furtunato, O.M., Medeiros, V.S., Almeida, I.S., 2011. Levantamento da geodiversidade. Projeto Atlas Pluviométrico do Brasil – isoietas anuais médias, período 1977 a 2006. CPRM, escala 1:1.000.000.

Sioli H., 1984. The Amazon and its main affluents: Hydrography, morphology of the river courses, and river types. In: Sioli H. (eds). The Amazon. Monographiae Biologicae vol 56, Springer, Dordrecht.

Steffen, D., Preusser, F., Schlunegger, F., 2009. OSL quartz age underestimation due to unstable signal components. Quaternary Geochronology 4(5), 353-362.

Tassinari, C.C.G., Bittencourt, J.S., Geraldes, M.C., Macambira, M.J.B., Lafon, J.M., 2000. The Amazon Craton. *In:* Cordani, U.G., Thomaz-Filho, A., Campos, D.A. (Eds.) Tectonic Evolution of South America. Acad. Bras. Cienc. Spec. Publ. 31st Int. Geol. Cong., pp. 41-95.

Viers, J., Roddaz, M., Filizola, N., Guyot, J-L., Sondag, F., Brunet, P., Zouiten, C., Boucayrand, C., Martin, F., Boaventura, G.R., 2008. Seasonal and provenance controls on Nd-Sr isotopic compositions of Amazon rivers suspended sediments and implications for Nd and Sr fluxes exported to the Atlantic Ocean. Earth and Planetary Science Letters 3-4, 511-523.

Wintle, A.G., Adamiec, G., 2017. Optically stimulated luminescence signals from quartz: A review. Radiation Measurements 98, 10-33.

Wittmann, H., von Blanckenburg, F., Guyot, J. L., Maurice, L., Kubik, P.W., 2009. From source to sink: Preserving the cosmogenic ^{10}Be-derived denudation rate signal of the Bolivian

Andes in sediment of the Beni and Mamoré foreland basins. Earth and Planetary Science Letters 288(3), 463-474.

Wittmann, H., von Blanckenburg, F., Maurice, L., Guyot, L., Filizola, N., Kubik, P.W., 2010. Sediment production and delivery in the Amazon River basin quantified by in situ–produced cosmogenic nuclides and recent river loads. Geological Society of America Bulletin B30317-1.

Zhang, Y., Chiessi, C.M., Mulitza, S., Sawakuchi, A.O., Häggi, C., Zabel, M., Schefuß, E., Crivellari, S., Wefer, G., 2017. Different precipitation patterns across tropical South America during Heinrich and Dansgaard-Oeschger stadials. Quaternary Science Reviews 177, 1-9.